We P1 12

Localised Time-lapse 3D Elastic Full Waveform Inversion Using Finite-difference Injection and Wavefield Extrapolation

S. Yuan* (Institut de Physique du Globe de Paris (IPGP)), N. Fuji (IPGP), D. Borisov (Princeton University) & S. Singh (IPGP)

SUMMARY

We present a novel methodology for inverting 3D elastic time-lapse data for local target structures of the Earth's interior. Since we are particularly interested in the small property change in a deep target region, we extrapolate sources and receivers on the Earth's surface to a virtual surface in the vicinity of the region of interest, in order to facilitate and stabilise full waveform inversion (FWI) scheme. The key is i) finite-difference injection method (FDIM) for source representation onto the small deep region; and ii) wavefield extrapolation (WE) for receiver side, which takes fully into account elastic behaviour outside the region. Here in this presentation, for the first time, we present the combination of FDIM and WE in order to perform time-lapse 3D elastic FWI for localised structures deep beneath the Earth's surface. This localised FWI allows us not only to significantly reduce computational costs and memory requirements, but also to stabilise inversions and avoid spurious model update. In this paper, we compare mainly the first gradients of the localised time-lapse 3D elastic FWI with those obtained by FWI for a whole area.

Introduction

Full waveform inversion (FWI) is a promising technique in providing quantitative and high-resolution images of subsurface structures. However, even on state-of-art computing devices, the high computational cost of 3D elastic FWI still hinders its wide applications to practical problems in oil industry. On the other hand, in time-lapse seismic surveys, such as reservoir monitoring or CO_2 injection, perturbations mainly occur within a certain small area while the large baseline model remains unchanged. It seems thus too much time- and resource- consuming to perform 3D elastic FWI for an entire model space, which we refer to as "full-model" FWI hereafter, while we just wish to extract information on the structure of the small target region that changes (e.g., the blue region in Figure 1a). Thence one expects to develop an intermediate (reasonable) FWI scheme applicable to the time-lapse experiments without loosing interest of using the resolving power of FWI. We thus propose a localised 3D elastic FWI in this paper, where we limit the region of FWI to be around the target region which changes with time actually. The underline assumption of localised FWI is that we know the baseline model and that it does not change at all. In order to realise the localised FWI, we propose to combine finite-difference injection method (FDIM) (Robertsson and Chapman, 2000; Borisov et al., 2015) and wavefield extrapolation (WE) in order to re-datum, where these two methods are equivalent to injecting sources and receivers onto subsurface (Figure 1b).

Our strategy is i) first to obtain within the region of interest the equivalent expression for the sources located outside the region of interest (FDIM); and ii) to extrapolate the waveform residual measured on the Earth's surface to the virtual surface located on the top of the target region (WE), as we explain in the following sections.

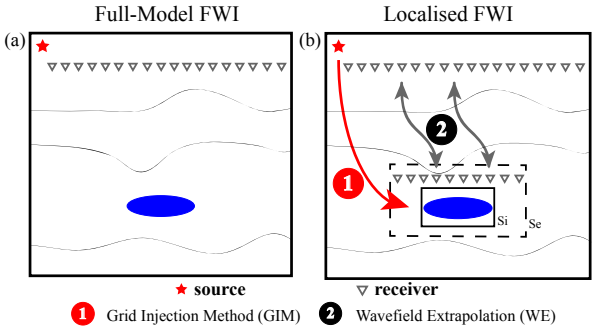

Figure 1 *Schematic illustration of full-model FWI and localised FWI. S_i denotes an injection boundary and S_e serves as an absorbing boundary. (a) Full-model FWI; (b) Localised FWI integrating FDIM and WE.*

Finiete-difference Injection Method (FDIM) - Localised Forward Simulation

FDIM is an efficient and robust tool for localised forward simulation under finite difference scheme without re-calculating the wavefield in unaltered model spaces (Robertsson and Chapman, 2000; Borisov et al., 2015; Monteiller et al., 2013). Generally speaking, it is equivalent to re-distributing physical sources onto subsurface and propagating waves within a certain smaller region. In terms of numerical simulations, we need to store the wavefield (i.e. velocity and stress) on a surface enclosing the area of interest. This enclosed surface, named as injection boundary (shown as a solid rectangle S_i in Figure 1b), will serve as the new boundary condition and act as sources for the subsequent localised forward modelling. The other dashed rectangle S_e shown in Figure 1b denotes a localised absorbing boundary so that the wavefield scattered inside S_e does not produce artifacts from the limits of new modelling region. When FDIM is applied to the identical model (without perturbation inside S_i), as shown in Figures 2a-d, the wavefield is accurately reconstructed. Figure 2b and 2c show the snapshots of wavefield calculated with full-model and localised FDIM methods, whereas Figure 2d shows the synthetics recorded at points inside the red circles in Figures 2b-c. It is clear that we do not see a significant difference between full-model and localised FDIM modelled synthetics. The wavefield outside injection boundary S_i remains zero since the model has not changed (Figure 2c).

When the model is perturbed (Figure 2e-l, oil/gas reservoir or CO_2 injection, etc.), wavefield has some scattered energy outside S_i (Figure 2g). When we compare the full-model and the localised synthetics for first arrivals (e.g., at 800 ms, see Figures 2f-h), we see that the wavefield is much alike even under the existence of perturbation inside S_i. However, when we keep on observing the later phases (e.g., at 1200 ms, see Figures 2j-l), we observe not only that no artificial reflections occur at the localised absorbing boundary S_e, but also that we thus cannot reproduce the high-order interactions between the scattered wavefield and outer structures (Figure 2l). Those differences are due to the higher-order interactions, but since it is relatively small and we are still interested in inverting first several significant phases, we do not really have to be worried about this effect in our methodology.

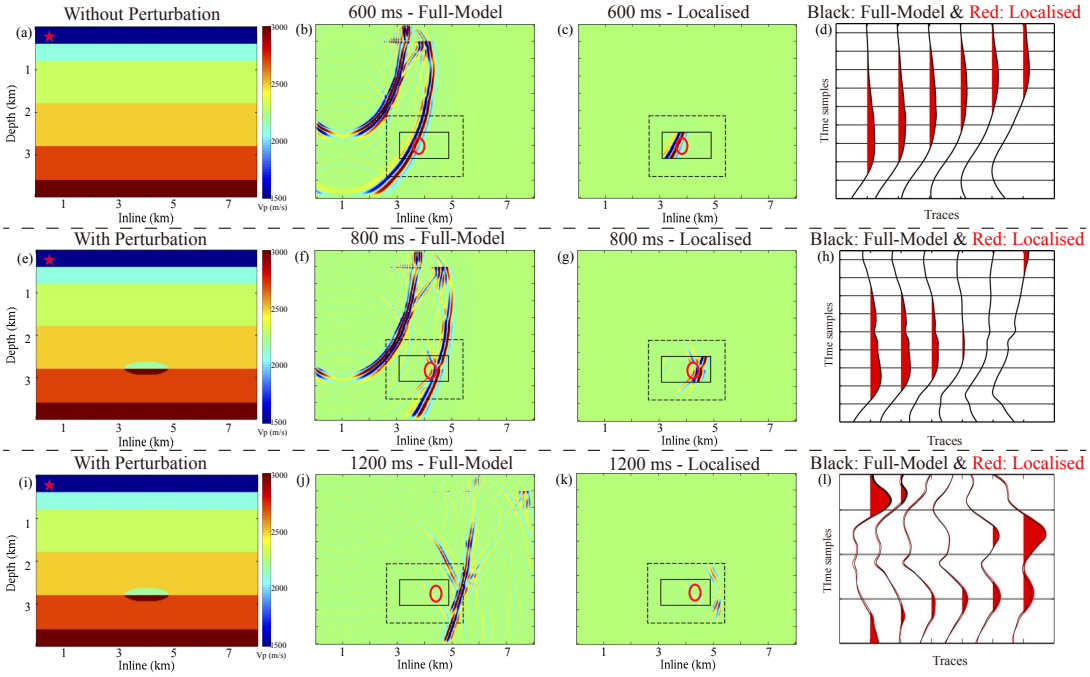

Figure 2 *Snapshots of V_z component using full-model and localised forward simulation. a-d) an identical model; e-l) a perturbed model; b) f) and j) snapshots with "full-model" calculation; c) g) and k) snapshots with FDIM; d) h) and l) synthetic comparison recorded at stations inside the red circle.*

Wavefield Extrapolation (WE) of waveform residuals recorded at the Earth's surface

WE deals with implementing virtual receivers inside the Earth by extrapolating waveform residuals collected at the Earth's surface, using the a priori information on the Earth's structure outside S_i (i.e., the baseline model). There exist various classical wavefield extrapolation methods such as Kirchhoff summation, phase-shift methods, which are in fact based on ray theory. However, it is not accurate enough for conducting the localised elastic FWI so we need to revisit the representation theorems so that we can extrapolate the waveform residuals to an arbitrary point inside the Earth, supposing that we know the baseline model. Omitting the details, one can obtain the representation theorem in frequency domain for the waveform residual measured on the Earth's surface (receivers' plane) $\partial\mathbb{D}_0$ to an arbitrary point $\mathbf{x}_B$ deep beneath $\partial\mathbb{D}_0$:

$$\delta d_n^*(\mathbf{x}_B,\mathbf{x}_A,\omega) = -\int_{\partial\mathbb{D}_0}\left[\delta\sigma_{ij}^*(\mathbf{x},\mathbf{x}_A)G_{in}(\mathbf{x},\mathbf{x}_B)+\delta d_i^*(\mathbf{x},\mathbf{x}_A)\Sigma_{ijn}(\mathbf{x},\mathbf{x}_B)\right]n_j\,dS, \tag{1}$$

where δd_n is the n-th component of waveform residual (in velocity) and $\delta\sigma_{ij}$ is the stress residual, whereas G_{in} denotes i-th component of velocity Green's function with n-th component single force and Σ_{ijn} denotes ij-th component of stress Green's function with n-th component single force. ω is angular frequency and $*$ denotes the complex conjugation. The associated stress component will be simplified to pressure wavefield under the fluid-solid boundary condition (Ravasi and Curtis, 2013) which is realisable through 4-components ocean bottom receivers. Figure 3 shows an example of extrapolated wavefield from a 3D profile and note that WE needs to be done only once prior to localised FWI.

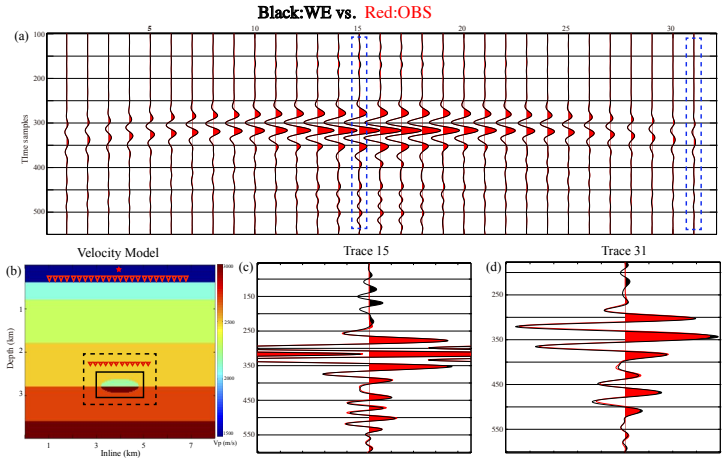

Figure 3 *Wavefield extrapolation examples. (a) The extrapolated wavefiled (black) and the true wavefield (red) on the virtual surface. (b) Shot configuration. (c), (d) The zoom-in waveforms of the selected two traces in (s).*

Localised FWI

After FDIM and WE, localised 3D elastic FWI is performed using classical formulation developed by Tarantola (1984). The difference between modelled and observed data was minimised iteratively in a least-square sense for each shot:

$$S = \sum_{\text{shots}} \int_0^T \sum_{\text{receivers}} [d_{mod}(t) - d_{obs}(t)]^2 \, dt \tag{2}$$

This objective function looks the same with traditional FWI. However, d_{mod} represents the simulated scattered waveform only depending on the target perturbations, while d_{obs} is extrapolated difference between baseline and time-lapse surveys. This strategy is similar to the so-called double-difference waveform inversion (Yang et al., 2015) which is more robust than standard time-lapse FWI. Forward simulation was achieved using finite difference scheme with staggered grid of fourth-order accuracy in space and second-order in time. The gradients for model update were obtained through adjoint-state technique (Plessix, 2006).

For the schematic illustration of localised FWI, we chose 8 km $\times$ 8 km $\times$ 4 km 3D elastic model without (baseline model) and with a lens-shaped perturbation to simulate time-lapse seismic surveys (figure 4a,b). The synthetic test consists 49 shots with a 1 km spacing interval. The source is a Ricker wavelet with dominant frequency at 6 Hz. Physical receiver plane consists of 161×161 4-C OBN/OBCs while the virtual plane consists of 56×56 with the same interval of 40 m.

We performed full-model and localised FWI for the first iteration to compare the computational efforts and the potential quality of FWI results. The computational effort of localised FWI is at least reduced with factor of 7 compared to full-model FWI due to the reduction of model size. The first gradient directions are consistent with each other. Since WE does not extrapolate residual wavefield with the same accuracy to every virtual receiver as we explained in the previous section, it is still under discussion how to weight extrapolated residuals. However, it is not also necessarily required that the gradient directions should be identical since the gradient obtained by full-model FWI does not have a good resolution in the deep part.

Conclusions and perspectives

We combine FDIM and WE for the first time in order to develop a novel methodology of localised waveform inversion for time-lapse 3D seismic surveys. It is shown that FDIM is efficient and robust enough even though the second or higher order scatter wavefield was neglected due to localised ab-

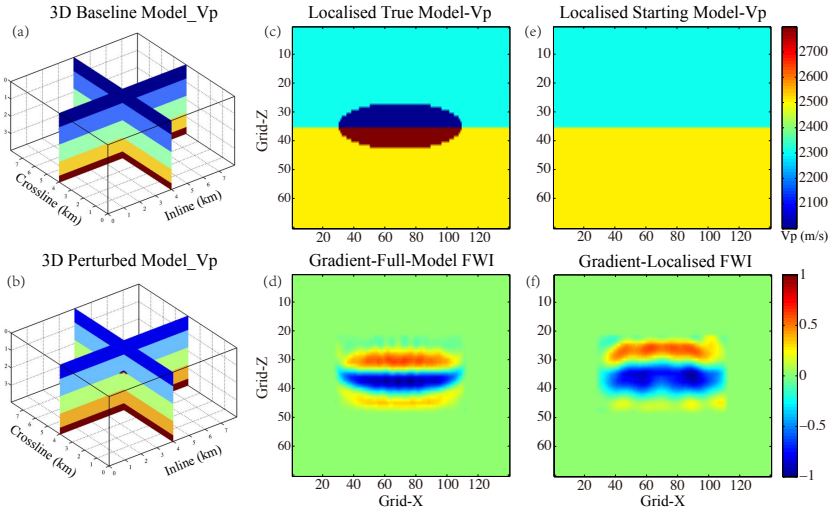

Figure 4 *First gradient of full-model FWI and localised FWI. (a) 3D Vp baseline model; (b) 3D Vp perturbed model; (c), (e) Localised true and starting Vp true model, respectively; (d), (f) First gradient of full-model and localised FWI.*

sorbing boundary. We succeeded in reconstructing both phase and amplitude by WE, as long as the shots-receivers geometry is well configured albeit some spurious events due to truncation problems. The developed localised FWI, which naturally focuses on the scattered wavefield due to perturbations within target regions, will not only contribute to reducing the computational and facilitate cost to a great extent, but also to avoiding the spurious model update outside target zones and suppressing non-repeatability effects of time-lapse surveys. Besides, the decrease of computational areas could help to enlarge the bandwidth of FWI, which will lead to a higher resolution. Based on preliminary results, we think the localised FWI is promising and the other advantages and limitations are still under investigation. However, more investigations should be performed in order to control the FWI image since it is influenced by WE quality.

Acknowledgments

We thank GPX consortium for funding this project. This work was performed using IPGP cluster.

References

Borisov, D., Singh, S.C. and Fuji, N. [2015] An efficient method of 3-D elastic full waveform inversion using a finite-difference injection method for time-lapse imaging. *Geophysical Journal International*, **202**(3), 1908–1922.

Monteiller, V., Chevrot, S., Komatitsch, D. and Fuji, N. [2013] A hybrid method to compute short-period synthetic seismograms of teleseismic body waves in a 3-D regional model. *Geophysical Journal International*, **192**(1), 230–247.

Plessix, R.E. [2006] A review of the adjoint-state method for computing the gradient of a functional with geophysical applications. *Geophysical Journal International*, **167**(2), 495–503.

Ravasi, M. and Curtis, A. [2013] Elastic imaging with exact wavefield extrapolation for application to ocean-bottom 4C seismic data. *Geophysics*, **78**(6), S265–S284.

Robertsson, J.O. and Chapman, C.H. [2000] An efficient method for calculating finite-difference seismograms after model alterations. *Geophysics*, **65**(3), 907–918.

Tarantola, A. [1984] Inversion of seismic reflection data in the acoustic approximation. *Geophysics*, **49**(8), 1259–1266.

Yang, D., Meadows, M., Inderwiesen, P., Landa, J., Malcolm, A. and Fehler, M. [2015] Double-difference waveform inversion: Feasibility and robustness study with pressure data. *Geophysics*, **80**(6), M129–M141.